Procedure Based on External Quantum Efficiency for Reliable Characterization of Perovskite Solar Cells

Lucia V. Mercaldo,* Eugenia Bobeico, Antonella De Maria, Marco Della Noce, Manuela Ferrara, Laura Lancellotti, Antonio Romano, Gennaro V. Sannino, Giuseppe Nasti, Antonio Abate, and Paola Delli Veneri

Perovskite solar cells (PSCs) have the potential for widespread application, but challenges remain for a reliable characterization of their performance. Standardized protocols for measuring and reporting are still debated. Focusing on the short circuit current density (J_{SC}), current–voltage characteristics (J–V) and external quantum efficiency (EQE) are collected to estimate the parameter. Still, they often provide a mismatch above 1 mA cm^{-2}, resulting in a possible 5% or higher error. Combining experimental data and optical simulations, it is demonstrated that the EQE can provide a reliable estimate of the J_{SC} that could otherwise easily be overestimated by J–V. With access to the internally transmitted light through simulations, an upper limit for EQE is defined depending on the front layers. Details on the origin of the spectral shape and contributions to the optical losses are obtained with further optical simulations, providing hints for cell optimization to achieve a photocurrent gain. The authors use solution-processed *n-i-p* PSCs with triple-cation mixed-halide absorbers as demonstrators and ultimately come to the proposal of an upgrade of the present best practices in PSC efficiency measurements. Still, the approach and conclusions are general and apply to cells with all designs and chemical formulations.

1. Introduction

Perovskite solar cells (PSCs), with their potential for application and relatively easy fabrication procedure by different routes (both solution- and vacuum-based), have attracted wide attention over the past decade.[1,2] Thanks to extensive efforts, the power conversion efficiency of PSCs has rapidly reached up to 25.7%,[3] thus competing with conventional photovoltaics, meanwhile generating an ever-increasing number of reports.[4]

PSC technologies are now facing stability and upscaling issues to make commercialization feasible.[5,6] Alongside, as PSCs present measurement challenges, there is increasing attention toward defining best practices for measuring and reporting their performance while also working toward standardized protocols.[7–13] In this context, the role of the external quantum efficiency (EQE) is debated. On the one hand, the EQE is among the standard characterization techniques for photovoltaic devices. The method provides detailed information on the solar cell, an estimate of the short-circuit current density (J_{SC}), and the establishment of the spectral mismatch factor in the J–V characterization under simulated sunlight.[12,13] On the other hand, a somewhat generalized discrepancy in current density was recently reported for PSCs, with the J_{SC} extracted from EQE consistently lower than the J_{SC} from J–V scans.[14] On this basis, a discussion and possible revision of the requirement for matched values from the two techniques was proposed.

Looking into literature data can be instructive in this context. Meaningful data from peer-reviewed articles published on PSCs have recently been collected in an extensive database and made available to the community for interactive exploration, analysis, and graphical representation.[4] Among the options, it is possible to focus on comparing solar cell metrics as a function of the bandgap of the perovskite absorber layer. **Figure 1**a–d reports

---

L. V. Mercaldo, E. Bobeico, A. De Maria, M. Della Noce, M. Ferrara,
L. Lancellotti, A. Romano, G. V. Sannino, P. Delli Veneri
Portici Research Center
Italian National Agency for New Technologies
Energy and Sustainable Economic Development (ENEA)
80055 Portici, NA, Italy
E-mail: lucia.mercaldo@enea.it

The ORCID identification number(s) for the author(s) of this article
can be found under https://doi.org/10.1002/ente.202200748.

G. V. Sannino
Department of Chemical Sciences
University of Naples Federico II
80126 Naples, Italy

G. Nasti, A. Abate
Department of Chemical, Materials and Production Engineering
University of Naples Federico II
80125 Naples, Italy

A. Abate
Department Novel Materials and Interfaces for Photovoltaic Solar Cells
Helmholtz-Zentrum Berlin für Materialien und Energie
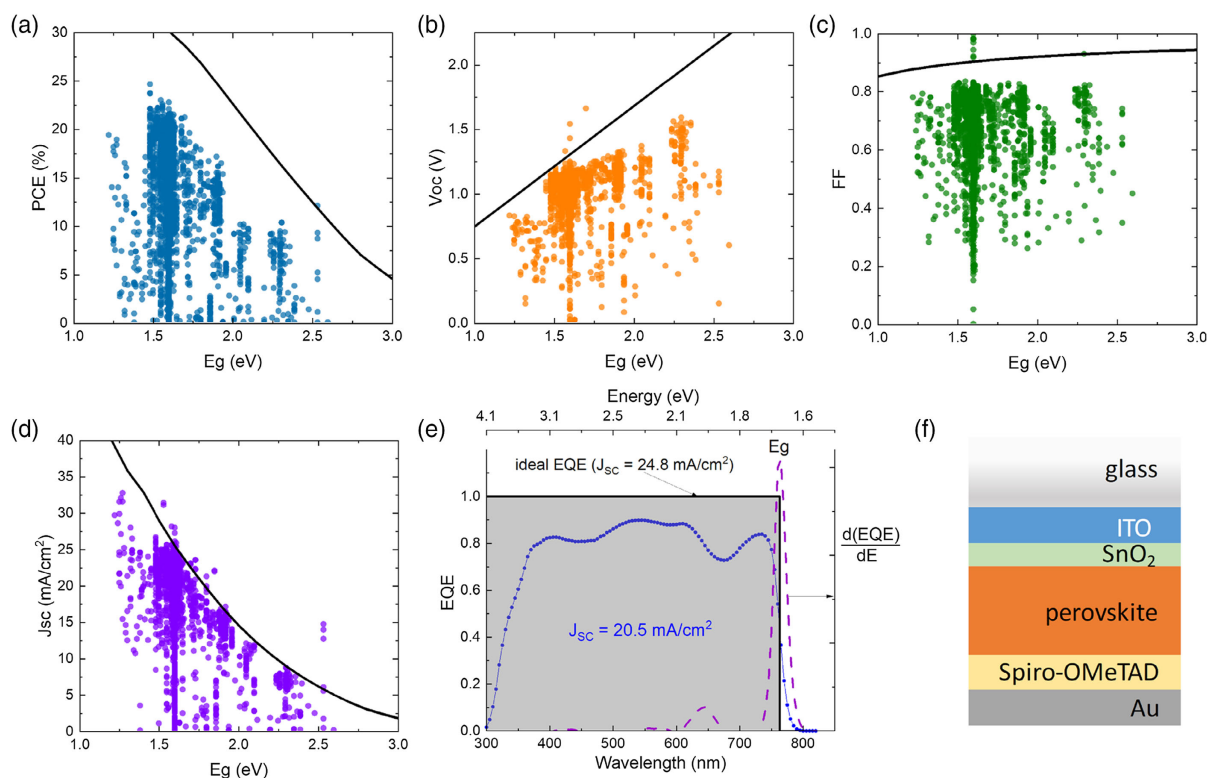14109 Berlin, Germany

ADVANCED
SCIENCE NEWS

www.advancedsciencenews.com

Energy Technology
Generation, Conversion, Storage, Distribution

www.entechnol.de

Figure 1. a–d) Bandgap dependence of the photovoltaic parameters of perovskite solar cells from recently published papers (data-range 2019–2021) as derived from the open perovskite database (https://perovskitedatabase.com)[4] using the available interactive tools, shown together with the ideal Shockley–Queisser limit for single-junction solar cells at standard test conditions[15] (black lines); e) ideal versus real external quantum efficiency (EQE) and bandgap estimate of one of our triple-cation perovskite solar cells; f) schematic structure of the perovskite solar cells here used as demonstrator.

the bandgap dependence of the photovoltaic parameters from recent articles (data range 2019–2021) as extracted from the database, shown together with the ideal Shockley–Queisser limit for single-junction solar cells at standard test conditions.[15] There is clear evidence that the J_{SC} parameter appears unreasonably close to the theoretical limit (black line in the figure) or even surpasses it in several cases. There could be different reasons for overestimated J_{SC}, such as an incorrectly calibrated solar simulator, imprecisions due to small device area (often well below 1 cm^2), and intrinsic features of PSCs that often present a dependence on scan rate, direction of J–V scans, and device preconditioning.[7,16–19] Requiring certification at accredited centers for every published efficiency would be impractical, while the availability of in-house reliable methods would be helpful. We here propose and validate an EQE-based procedure accessible to R&D labs for a reliable estimate of J_{SC} and, ultimately, cell efficiency. The present protocols use the EQE mainly as a benchmark for validation of J–V data, with mismatches even up to 20% tolerated.[7,14] Such large tolerance opens for a significant error on J_{SC}. Our procedure, developed to minimize this error, promotes the EQE to a primary role. The method is based on acquiring EQE spectra at low frequency (in the range of tens of Herz) and comparing experimental data with simple optical simulations. We here use as demonstrator *n-i-p* solar cells with lead-based mixed-cation (Cs, FA, MA) mixed-halide (I, Br) absorber,

a primarily studied composition also because of tandem applications,[20,21] SnO$_2$ as electron transport layer (ETL), and Spiro-OMeTAD as hole transport layer (HTL). However, the procedure is general, best suited to the vast class of PSCs that have demonstrated very high internal quantum efficiency, up to unity, and all the PSCs with EQE dictated by optical phenomena only, where very high currents (and efficiency records) are feasible. The procedure is still helpful for cells with relevant collection issues impacting the EQE as it provides realistic upper limits.

2. Results and Discussion

We start with brief considerations on the challenges, specific for PSCs, in the evaluation of J_{SC} from J–V characterization, including a concrete example. Next, we switch to the essentials of the EQE, and afterward move to the experiments and simulations carried out in this work.

Solar cells are primarily described and compared in terms of the photovoltaic parameters extracted from J–V scans under simulated sunlight: J_{SC}, open-circuit voltage (V_{OC}), and fill factor (FF), whose product, divided by the input power, furnishes the conversion efficiency of incident solar radiation to electrical power. PSCs feature a complex, dynamic response to changes in applied voltage during the J–V scans even in apparently

**ADVANCED
SCIENCE NEWS**

www.advancedsciencenews.com

Energy Technology
Generation, Conversion, Storage, Distribution

www.entechnol.de

''hysteresis-free'' devices.[9,16] This peculiarity of PSCs offers an unparalleled opportunity to study interesting physical behaviors and their origin, while finding methods for mitigating the transient phenomena.[17–19,22,23] At the same time, this makes for a major challenge for accurately determining the photovoltaic parameters of PSCs due to transient responses. Standardized protocols are not yet available for PSCs, but the test conditions should evidently provide a response reflecting the actual application of the device, or steady-state performance. Recommended best practices include the execution of asymptotic J–V scans (so-called dynamic J–V scans), waiting at each voltage step long enough to obtain the stabilized current output, and the maximum power point tracking.[9,11,13,16] Other major concerns are related to the simulated sunlight spectrum. Typically, a certified silicon solar cell is used for calibrating the intensity of the sun simulator light according to the AM1.5 g (Air Mass 1.5 global) standard spectrum with integrated power of 100 mW cm^{-2}. The much lower bandgap of silicon versus perovskites of the main compositions can easily lead to erroneous determination of J_{SC} even when using solar simulators with high-class spectra.[24] An instructive example is shown in the Supporting Information (Figures S1, S2 and Table S1, Supporting Information), together with the J–V curve of one of our triple-cation PSCs before and after applying the mismatch factor for data correction.

Adopting proper J–V scan conditions is crucial for a reliable estimate of the photovoltaic parameters. Taking spectral mismatches into account is equally relevant.[12,13,24] The mismatch factor accounts for the error caused by the spectral discrepancy between the simulator spectrum and the AM1.5g spectrum considering the reference and test cell spectral responses (details are in the Experimental Methods in the Supporting Information). The inputs are the irradiance of the standard spectrum, the irradiance of the simulator, and the EQEs of the test cell and reference cell (transformed into the spectral response), paired in products as integrands in both numerator and denominator of a fraction so that only relative values are required. Measuring the EQE is thus necessary to establish the spectral mismatch factor, and relative values are enough in this case. If absolute EQE is available, an alternative estimate of J_{SC} can also be derived, with the advantage of independence from the spectral shape of the illumination source, cell area, and J–V scan rates. By definition, the EQE measures the fraction of the incident photons that are harvested and converted into collected charge carriers at each wavelength. By multiplying with the AM1.5g photon flux at each wavelength, the flow of collected charges at that wavelength is obtained, and the integral over the entire spectral range gives the J_{SC} value. Besides this quantification, the EQE spectrum also provides essential information about the solar cell, based on how the spectral shape departs from the ideal EQE. Ideally, the quantum efficiency has a square shape (Figure 1e), being equal to one for photon energies above the absorber bandgap and zero for lower energies, due to the inability of the semiconductor to absorb photons with energies below the bandgap. The ideal J_{SC} limit is obtained as the integral of the product of the ideal EQE and the AM1.5g photon flux. Figure 1e, together with the ideal EQE, shows the experimental EQE of one of our solar cells with the architecture schematized in Figure 1f. In actual solar cells, the square shape is distorted mostly due to optical losses, primarily consisting of reflection losses and parasitic

absorption from the supportive layers (transport and contact layers). Due to collection issues and recombination, electrical losses may also affect the EQE shape. Therefore, the inspection of the EQE spectral shape can provide information about loss mechanisms into play in the solar cell, especially in comparative studies, together with access to an estimate of the bandgap of the absorber material within the device (in Figure 1e the method of the inflection point of EQE(E) is applied).[25] Quantitatively, in the present example, a bandgap of 1.62 eV, in agreement with the expected value based on the composition, and a J_{SC} of 20.5 mA cm^{-2} are extracted, with J_{SC} well below the ideal value of 24.8 mA cm^{-2} and below numerous reported values in the literature for the same bandgap (Figure 1d). We conducted an experimental investigation and an in-depth optical simulation study to establish the reliability of the J_{SC} values extracted from EQE for PSCs, often referred to as underestimating the outcomes of J–V scans.

The EQE technique typically uses a probe beam modulated by an optical chopper that triggers the detection with a lock-in amplifier. Operation in continuous monochromatic irradiation (DC mode) is another option. For absolute EQE measurements, the entire beam is focused within the device area to have a known intensity hitting the sample. Calibration is firstly performed using a detector of known responsivity. The intensity of the probe light at a given wavelength is low compared to one sun illumination. Still, a white light bias can also be applied, with the chopped monochromatic light representing only a small perturbation. For reliable measurement, the modulation frequency needs to be much lower than the frequency associated with all the mechanisms influencing charge carrier collection (generation, recombination, trapping/release, etc.).[26] The typical frequency of a few hundred Hz is generally inappropriate for PSCs due to their long response time scale.[14] Strong frequency dependence of the EQE of PSCs has been reported in some cases.[26] This means that measurement conditions might have to be readjusted depending on device type, materials, and interfaces.

We measured the EQE in different conditions and **Figure 2**a summarizes the results of our screening for one of the solar cells. For completeness, J–V characteristics and photovoltaic parameters for this solar cell are reported in Figure 2b and Table S1, Supporting Information (Figure S2, Supporting Information, also displays the solar simulator spectrum, while Figure S1, Supporting Information, shows the implications on the J–V data when the same cell is measured under a different spectrum).

The experiment shows variation among the different runs. The sequence of the measurements followed the order shown in the legend (from the top as first to bottom as last). The time evolution of the measured EQE in the various conditions allows for ruling out the possible deterioration of the perovskite or contact materials. At high frequency (583 Hz), appropriate for silicon solar cells, extremely low magnitude is obtained unless white light bias is applied, setting the cell closer to realistic operating conditions. The dependence on light bias and chopper frequency is connected to the physics of the device with a possible contribution from a wide variety of mechanisms, like trap-state filling, different recombination processes, space-charge effects, and others.[12] One possible explanation for the observed trend is based on trap-state filling with a long response time (compared
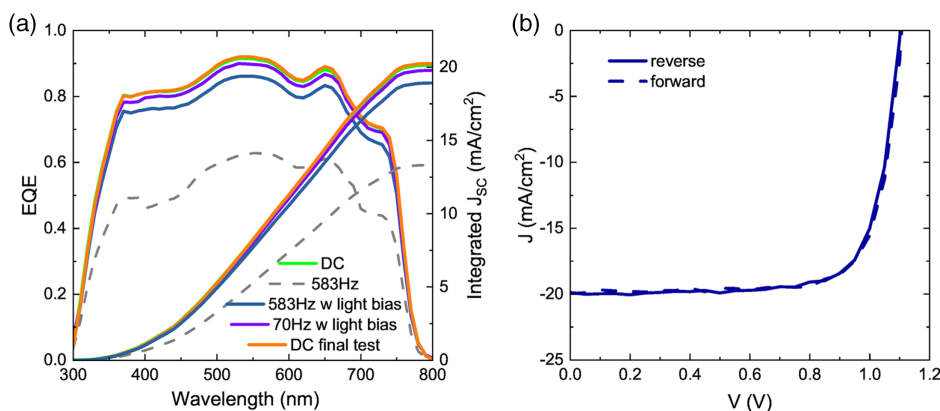
ADVANCED
SCIENCE NEWS
www.advancedsciencenews.com

Energy Technology
Generation, Conversion, Storage, Distribution
www.entechnol.de

Figure 2. a) EQE spectra (left axis) of a triple cation perovskite solar cell measured in different conditions and integrated J_{SC} values (right axis); b) J–V scans under simulated sunlight of the same device (the simulator spectrum is shown in Figure S2, Supporting Information).

to the measurement frequency) and the different impact when charge density in the device is varied (with versus without light bias). When close to dark conditions, the few photogenerated charge carriers likely suffer from trapping/release, hence the low response. When light bias is applied, the continuous photogeneration saturates the traps preventing the carriers generated by the chopped light from being trapped. The continuous light bias thus mitigates the long response time effects, but the modulation frequency has still to be adapted to the device under test. Figure 2a shows that higher EQE is measured over the entire wavelength range, reducing it to 70 Hz while keeping the light bias. This indicates a relatively slow response that requires a reduced chopper frequency to avoid measurement artifacts. A comparable or even slightly higher response is observed when measuring in DC mode. In the above trap-filling picture, this could be ascribed to the continuous illumination with monochromatic light that, similarly to the light bias, allows overcoming the trapping effects, as already reported for dye-sensitized solar cells.[27]

Regardless of the origin of the slow response, which goes beyond the scope of this work, we here want to adopt a practical point of view in the context of solar cell characterization. The indications from the present experiment are that a frequency of ≈70 Hz with the application of white light bias or DC mode should be appropriate measurement settings. Figure 2 shows, in fact, good agreement between EQE and J–V scans. Low-frequency values of 10–20 Hz often provide good conditions even without white light bias, with matched J_{SC} from J–V and EQE, as shown in Figure S3, Supporting Information, for a lead-free PSC.[28–31] In this additional experiment, a different multimodal characterization set-up was integrated into a glovebox due to the extreme instability of Sn-based perovskite, and the EQE was measured at 16 Hz without light bias. Nevertheless, due to the strong dependence on test conditions for both J–V scans and EQE, it would be helpful to have a realistic upper limit for the EQE.

We propose to disclose a realistic reference for the EQE using an essential optical simulation study, by evaluating the internal transmittance of the front stack into the perovskite absorber. We used the free software IMD for optical modeling of multilayer films[32] as a simulation tool, but several other equivalent tools

are available. We simulated the two simple structures shown in **Figure 3**a,b (for generality concerns, an additional example for a different layer sequence is reported in Figure S4, Supporting Information). The layers were modeled using complex refractive indices and thickness values experimentally determined by spectroscopic ellipsometry[21] (183 nm for ITO and 29 nm for SnO_2 in Figure 3c).

The simulation of the stack in Figure 3a allows direct comparison with the experimental transmittance of the bilayer sample on glass. The simulated transmittance is reported as a solid black line in Figure 3c. The excellent agreement with the experimental transmittance (curve shown with symbols) supports the validity of the procedure. The simulation of the stack in Figure 3b provides access to the not-measurable internal transmittance into the perovskite, i.e., the actual light that reaches the absorber layer and is available for carrier generation. The calculated transmittance shows a maximum of 91.7% at 535 nm, and the average transmittance in the 450–800 nm range is slightly increased with respect to the transmittance into the air. This is thanks to the increased in-coupling of light into the active layer for the favorable index matching of light traveling from the window layers ($n \approx 1.8 - 2$) to perovskite ($n \approx 2.5$) vs air ($n = 1$), as thoroughly discussed in recent work.[33] The transmittance maximum is strongly dependent on the thickness of the front layer stack, shifting to higher wavelengths for increasing ITO thickness (Figure 3d).

The calculated transmittance is the actual upper limit for the EQE. We have then compared the measured EQE with the simulated transmittance. The comparison is shown in **Figure 4**a for two similar cells with a slight variation of layer thicknesses, measured with the two methods described earlier (70 Hz with white light bias and DC mode). Good agreement is observed in the spectral region where the active layer is strongly absorbing (up to ≈600 nm). This practically means that all the light that reaches the absorber layer generates photocarriers and these are collected at the electrodes, essentially with no losses. Larger EQE values, required for extracting a presumably larger J_{SC}, would not be physically possible, at least in this wavelength range. At longer wavelengths, the limited thickness and absorption coefficient of the absorber layer in the solar cell
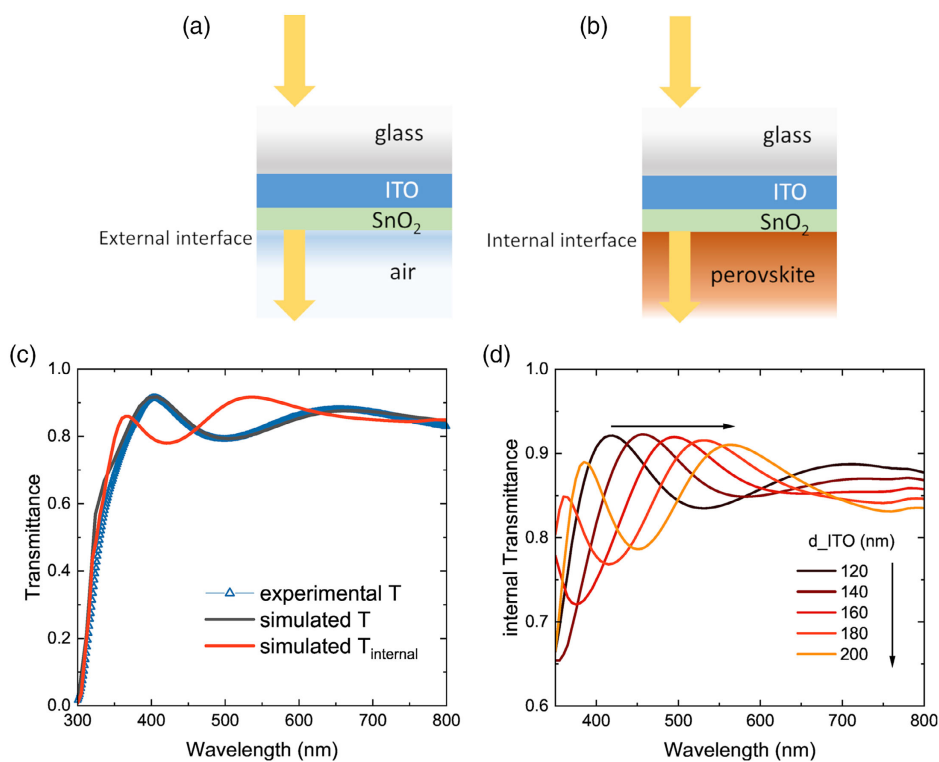
Figure 3. a,b) Modeled layer sequences; c) simulated transmittance of glass/ITO/SnO$_2$ into the air (black line) and into perovskite (red line) compared to the experimental transmittance of the stack measured with a spectrophotometer (symbols); d) Simulated internal transmittance with the variation of ITO thickness.
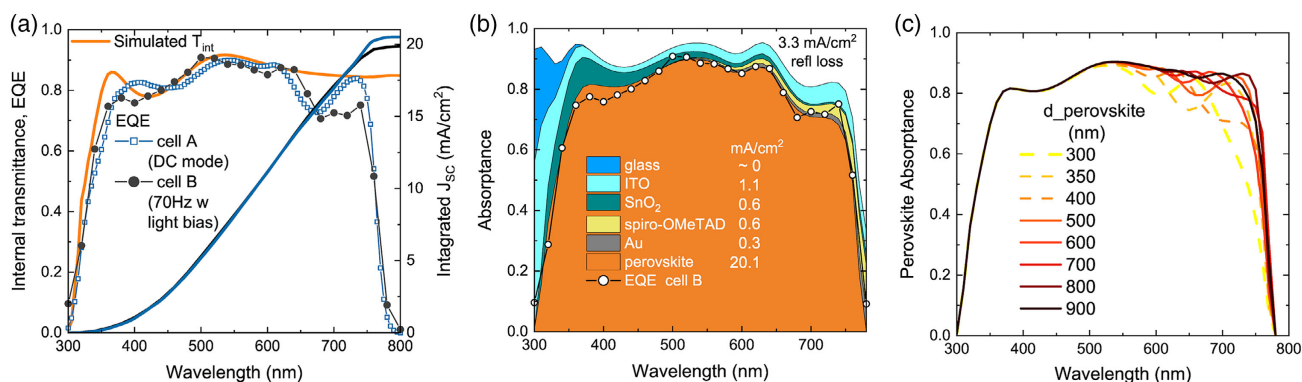

Figure 4. a) EQE spectra measured for two similar solar cells compared to the simulated internal transmittance; b) results of the optical simulation of the entire device stack and comparison with EQE data of cell B of the panel a), with reported calculated short circuit current density and detail of the contribution of each layer to the optical losses in equivalent photocurrent density; c) simulated perovskite absorptance (equivalent to EQE in the absence of charge collection losses) for different perovskite layer thicknesses.

becomes relevant in shaping the EQE spectrum, while in the simulated structure the perovskite layer is modeled as an output medium. In our case, with perovskite layer thickness of ≈400 nm, the long-wavelength light is partially transmitted by the active layer. This makes the contribution of all the layers in the stack relevant for the optical description of the solar cell.

The discussed basic optical simulation already gives clear indications of the validity of the measured EQE. For validation in the full spectral range, we carried out an optical simulation of the entire device stack, as in Figure 1f, with the GenPro4 software.[34] In this case, it is possible to calculate the absorptance in the perovskite layer, which can be compared with the entire experimental EQE spectrum. The complete optical analysis additionally allows identifying the contributions from the various layers to the spectral shape, the loss contributions of each layer, and getting insights into possible strategies for J_{SC} enhancement by playing with layer thicknesses, together with practical J_{SC} limits for the

**ADVANCED
SCIENCE NEWS**

www.advancedsciencenews.com

Energy Technology
Generation, Conversion, Storage, Distribution

www.entechnol.de

selected cell structure. The simulation results when using realistic thicknesses, based on measurements on single layers, are shown in Figure 4b. We assumed flat interfaces, typical for planar PSCs, in agreement with the strong interference fringes in the spectra that imply negligible scattering effects. The calculated absorbance in the perovskite layer is compared to the experimental EQE of cell B and good agreement is found. Therefore, the complete optical simulation confirms the validity of the measured EQE in the entire spectral range. The agreement can also be seen as evidence of minimal electrical losses in the solar cell. The main losses have an optical origin, with all the calculated contributions reported in the figure in equivalent photocurrent density. The significant reflection loss ($3.3 \, \mathrm{mA \, cm^{-2}}$) can be easily mitigated by implementing an antireflection layer over the front side of the glass substrate. Both the transport layers contribute with $\approx 0.6 \, \mathrm{mA \, cm^{-2}}$ each, while ITO with $1.1 \, \mathrm{mA \, cm^{-2}}$.

The simulation also allows examining the impact of the perovskite layer thickness on the spectral shape of the EQE. Figure 4c shows the simulated absorbance for thickness varied between 300 and 900 nm, manifesting a strong spectral variation in the long-wavelength range due to interference effects. Variation in the interference fringes at long-wavelength is similarly observed when changing the HTL thickness (not shown). With such a strong dependence of the cell spectral response on layer thicknesses, careful optimization is required to maximize the short-circuit current. On this matter also, optical simulations can be of big help to get valuable suggestions accompanied by estimates of possible J_{SC} gain. Practical examples are illustrated in Figure S5, Supporting Information.

We now want to refocus on the consistency of the J_{SC} values from EQEs for PSCs. The characterization of PSCs is tricky and this also holds for EQE measurements. However, we have demonstrated that the screening of the measurement conditions (chopper frequency and light bias) accompanied by a simple optical simulation of the front stack allows access to a reliable J_{SC} value. On this basis, to avoid or minimize errors when evaluating and reporting the J_{SC} parameter, we suggest upgrading the current best practices in PSC characterization in the laboratories, with the EQE as a primary tool more than a reference only. The proposed procedure follows the steps illustrated earlier for validating the measured EQE: 1) select appropriate EQE measurement conditions (low frequency in the tens of Hertz range, generally with white light bias, or DC mode if available); 2) Measure the EQE and check for reproducibility when repeating the measurement (to rule out degradation issues); 3) Calculate the mismatch factor M and apply it to correct the J–V data ($J_{corrected} = J_{measured} \, \mathrm{M}^{-1}$); 4) In case of discrepancy between J_{SC} values from J–V and EQE, simulate the internal transmittance of the front stack to set the upper limit for the EQE and validate the measured spectrum (some remarks are reported in the Supporting Information); this would have to be repeated when cells with a new front stack are measured; 5) Once the EQE data is validated, use the integrated current to calculate the corrected efficiency of the PSC under test.

The measured EQE should ideally reach the internal transmittance spectra. This is now the case for a wide variety of PSCs where major collection issues have been solved and the EQE is dominated by optical phenomena only. The proposed procedure works at its best with all these cells, which are also the cases

where very high currents are feasible, and errors on measured currents may yield values that even surpass the theoretical limit. When the measured EQE does not reach the internal T in the comparison, the main reasons could be that the optimal measurement conditions were not found, the cell degrades while being measured, and electrical issues still impact the EQE. This is the case of the lead-free PSC in Figure S3, Supporting Information, where the EQE maximum is 0.72 only, evidently below what could be reasonably expected based on optics. Here, collection issues are still likely impacting the cell spectral response. This could be related to the well-known high defect density of the Sn-based perovskite absorber due to Sn^{2+} to Sn^{4+} oxidation that causes p-type self-doping, and to the energy-band misalignment between the absorber and extracting layers, which also reflects in the low V_{OC} of the devices.[35,36] Even in such cases, the procedure could still be helpful as it would provide a realistic limit to aim to, for the EQE and thus for J_{SC} (Figure S6, Supporting Information). For specific cell designs with the use of thick front electrode or textured antireflection foils, the procedure is still feasible with suited software (GenPro4 or other).

3. Conclusion

We have observed that the J_{SC} of PSCs can be easily overestimated. Combining experimental data and optical simulations, we have demonstrated that the EQE can deliver a reliable estimate of J_{SC}. We have thus proposed a procedure for minimizing errors in J_{SC}, with the EQE playing a central role, and provided a best practice list for a practical implementation manageable in R&D labs. In its more complete version, the procedure includes the execution of optical simulations, here illustrated to validate the method. As a complementary product, optical simulations can serve as a helpful guidance for device optimization. We have shown that optical analysis helps indeed with providing indications on ways to tune the spectral shape of the EQE for increased J_{SC} by playing with layer thicknesses. In particular, the thickness of the front transparent electrode gives the means to adjust the position of the spectral response maximum, while the thicknesses of the perovskite absorber and rear transport layer impact the long-wavelength fringes. The illustrated procedures can be repeated for other cell types, and the results are general.

Supporting Information

Supporting Information is available from the Wiley Online Library or from the author.

Acknowledgements

Conflict of Interest

The authors declare no conflict of interest.

Data Availability Statement

The data that support the findings of this study are available from the corresponding author upon reasonable request.

Keywords

[1] S. D. Stranks, H. J. Snaith, *Nat. Nanotech.* **2015**, *10*, 391.

[2] J. Jeong, M. Kim, J. Seo, H. Lu, P. Ahlawat, A. Mishra, Y. Yang, M. A. Hope, F. T. Eickemeyer, M. Kim, Y. J. Yoon, I. W. Choi, B. P. Darwich, S. J. Choi, Y. Jo, J. H. Lee, B. Walker, S. M. Zakeeruddin, L. Emsley, U. Rothlisberger, A. Hagfeldt, D. S. Kim, M. Grätzel, J. Y. Kim, *Nature* **2021**, *592*, 381.

[3] M. A. Green, E. D. Dunlop, J. Hohl-Ebinger, M. Yoshita, N. Kopidakis, K. Bothe, D. Hinken, M. Rauer, X. Hao, *Prog. Photovolt.* **2022**, *30*, 687.

[4] T. J. Jacobsson, A. Hultqvist, A. García-Fernández, A. Anand, A. Al-Ashouri, A. Hagfeldt, A. Crovetto, A. Abate, A. G. Ricciardulli, A. Vijayan, A. Kulkarni, A. Y. Anderson, B. P. Darwich, B. Yang, B. L. Coles, C. A. R. Perini, C. Rehermann, D. Ramirez, D. Fairen-Jimenez, D. Di Girolamo, D. Jia, E. Avila, E. J. Juarez-Perez, F. Baumann, F. Mathies, G. S. A. González, G. Boschloo, G. Nasti, G. Paramasivam, G. Martínez-Denegri, et al., *Nat. Energy* **2022**, *7*, 107.

[5] J. Yan, T. J. Savenije, L. Mazzarella, O. Isabella, *Sustain. Energy Fuels* **2022**, *6*, 243.

[6] S. H. Reddy, F. Di Giacomo, A. Di Carlo, *Adv. Mater.* **2022**, *12*, 2103534.

[7] J. A. Christians, J. S. Manser, P. V. Kamat, *J. Phys. Chem. Lett.* **2015**, *6*, 852.

[8] E. Zimmermann, K. K. Wong, M. Müller, H. Hu, P. Ehrenreich, M. Kohlstädt, U. Würfel, S. Mastroianni, G. Mathiazhagan, A. Hinsch, T. P. Gujar, M. Thelakkat, T. Pfadler, L. Schmidt-Mende, *APL Mater.* **2016**, *4*, 091901.

[9] R. B. Dunbar, B. C. Duck, T. Moriarty, K. F. Anderson, N. W. Duffy, C. J. Fell, J. Kim, A. Ho-Baillie, D. Vak, T. Duong, Y. Wu, K. Weber, A. Pascoe, Y.-B. Cheng, Q. Lin, P. L. Burn, R. Bhattacharjee, H. Wang, G. J. Wilson, *J. Mater. Chem. A* **2017**, *5*, 22542.

[10] IEC TR 63228:2019, *Measurement Protocols for Photovoltaic Devices Based on Organic, Dye-Sensitized or Perovskite Materials.*

[11] M. V. Khenkin, E. A. Katz, A. Abate, G. Bardizza, J. J. Berry, C. Brabec, F. Brunetti, V. Bulović, Q. Burlingame, A. Di Carlo, R. Cheacharoen, Y.-B. Cheng, A. Colsmann, S. Cros, K. Domanski, M. Dusza, C. J. Fell, S. R. Forrest, Y. Galagan, D. Di Girolamo, M. Grätzel, A. Hagfeldt, E. von Hauff, H. Hoppe, J. Kettle, H. Köbler, M. S. Leite, S. F. Liu, Y.-L. Loo, J. M. Luther, et al., *Nat. Energy* **2020**, *5*, 35.

[12] S.-H. Jeong, J. Park, T.-H. Han, F. Zhang, K. Zhu, J. S. Kim, M.-H. Park, M. O. Reese, S. Yoo, T.-W. Lee, *Joule* **2020**, *4*, 1206.

[13] T. Song, D. J. Friedman, N. Kopidakis, *Adv. Mater.* **2021**, *11*, 2100728.

[14] M. Saliba, L. Etgar, *ACS Energy Lett.* **2020**, *5*, 2886.

[15] S. Rühle, *Sol. Energy* **2016**, *130*, 139.

[16] M. Saliba, M. Stolterfoht, C. M. Wolff, D. Neher, A. Abate, *Joule* **2018**, *2*, 1019.

[17] B. Chen, M. Yang, S. Priya, K. Zhu, *J. Phys. Chem. Lett.* **2016**, *7*, 905.

[18] D.-H. Kang, N.-G. Park, *Adv. Mater.* **2019**, *31*, 1805214.

[19] P. Liu, W. Wang, S. Liu, H. Yang, Z. Shao, *Adv. Mater.* **2019**, *9*, 1803017.

[20] A. Al-Ashouri, E. Köhnen, B. Li, A. Magomedov, H. Hempel, P. Caprioglio, J. A. Márquez, A. B. M. Vilches, E. Kasparavicius, J. A. Smith, N. Phung, D. Menzel, M. Grischek, L. Kegelmann, D. Skroblin, C. Gollwitzer, T. Malinauskas, M. Jošt, G. Matič, B. Rech, R. Schlatmann, M. Topič, L. Korte, A. Abate, B. Stannowski, D. Neher, M. Stolterfoht, T. Unold, V. Getautis, S. Albrecht, *Science* **2020**, *370*, 1300.

[21] L. V. Mercaldo, E. Bobeico, A. De Maria, M. Della Noce, M. Ferrara, V. La Ferrara, L. Lancellotti, G. Rametta, G. V. Sannino, I. Usatii, P. Delli Veneri, *Energies* **2021**, *14*, 7684.

[22] F. Ebadi, N. Taghavinia, R. Mohammadpour, A. Hagfeldt, W. Tress, *Nat. Commun.* **2019**, *10*, 1574.

[23] N. E. Courtier, J. M. Cave, J. M. Foster, A. B. Walker, G. Richardson, *Energy Environ. Sci.* **2019**, *12*, 396.

[24] S. Ye, B. Chen, Y. Cheng, M. Feng, H. Rao, Y. M. Lam, T. C. Sum, *J. Phys. Chem. Lett.* **2020**, *11*, 3782.

[25] R. Carron, C. Andres, E. Avancini, T. Feurer, S. Nishiwaki, S. Pisoni, F. Fu, M. Lingg, Y. E. Romanyuk, S. Buecheler, A. N. Tiwari, *Thin Solid Films* **2019**, *669*, 482.

[26] S. Ravishankar, C. Aranda, P. P. Boix, J. A. Anta, J. Bisquert, G. Garcia-Belmonte, *J. Phys. Chem. Lett.* **2018**, *9*, 3099.

[27] P. M. Sommeling, H. C. Rieffe, J. A. M. van Roosmalen, A. Schönecker, J. M. Kroon, J. A. Wienke, A. Hinsch, *Sol. Energy Mater. Sol. Cells* **2000**, *62*, 399.

[28] G. Nasti, A. Abate, *Adv. Mater.* **2020**, *10*, 1902467.

[29] D. Di Girolamo, J. Pascual, M. H. Aldamasy, Z. Iqbal, G. Li, E. Radicchi, M. Li, S.-H. Turren-Cruz, G. Nasti, A. Dallmann, F. De Angelis, A. Abate, *ACS Energy Lett.* **2021**, *6*, 959.

[30] J. Pascual, G. Nasti, M. H. Aldamasy, J. A. Smith, M. Flatken, N. Phung, D. D. Girolamo, S.-H. Turren-Cruz, M. Li, A. Dallmann, R. Avolio, A. Abate, *Mater. Adv.* **2020**, *1*, 1066.

[31] G. Li, Z. Su, M. Li, F. Yang, M. H. Aldamasy, J. Pascual, F. Yang, H. Liu, W. Zuo, D. Di Girolamo, Z. Iqbal, G. Nasti, A. Dallmann, X. Gao, Z. Wang, M. Saliba, A. Abate, *Adv. Mater.* **2021**, *11*, 2101539.

[32] IMD *can be run as an extension to the free XOP software package, available at ESRF:* https://www.esrf.fr/home/UsersAndScience/support-and-infrastructure/software/data-analysis/OurSoftware/xop2.4/extensions.html

[33] K. O. Brinkmann, T. Becker, F. Zimmermann, C. Kreusel, T. Gahlmann, T. Haeger, T. Riedl, *Sol. RRL* **2021**, *5*, 2100371.

[34] R. Santbergen, T. Meguro, T. Suezaki, G. Koizumi, K. Yamamoto, M. Zeman, *IEEE J. Photovolt.* **2017**, *7*, 919.

[35] X. Jiang, F. Wang, Q. Wei, H. Li, Y. Shang, W. Zhou, C. Wang, P. Cheng, Q. Chen, L. Chen, Z. Ning, *Nat. Commun.* **2020**, *11*, 1245.

[36] X. Zhang, S. Wang, W. Zhu, Z. Cao, A. Wang, F. Hao, *Adv. Funct. Mater.* **2022**, *32*, 2108832.